Dalton Transactions

Accepted Manuscript

ROYAL SOCIETY OF CHEMISTRY

www.rsc.org/dalton

New Di-Ferrocenyl-Ethynylpyridinyl Triphenylphosphine Copper Halide Complexes and related Di-Ferricenyl Electro-crystallized Materials

Hakikulla H. Shah,[a] Rayya A. Al-Balushi,[a] Mohammed K. Al-Suti,[a] Muhammad S. Khan,[a,*] Frank Marken,[b,*] Anna L. Sudlow,[b] Gabriele Kociok-Köhn,b Christopher H. Woodall,[b] Paul R. Raithby[a,*] and Kieran C. Molloy[a,*]

[a]Department of Chemistry, Sultan Qaboos University, P.O. Box 36, Al-Khoudh 123, Sultanate of Oman

[b]Department of Chemistry, University of Bath, Bath, BA2 7AY, UK.

Three new neutral di-ferrocenyl-ethynylpyridinyl copper complexes, $[L_2(CuCl)_2(PPh_3)_2]$ (**2**), $[L_2(CuBr)_2(PPh_3)_2]$ (**3**), and $[L_2(CuI)_2(PPh_3)_2]$ (**4**) were synthesized from the ferrocenyl-ethynylpyridine ligand (L) (**1**), the appropriate copper halide CuX (with X = Cl^-, Br^-, I^-) and triphenylphosphine. These neutral complexes were fully characterized by spectroscopic methods and by single crystal X-ray crystallography. Cyclic voltammetry in dichloroethane revealed chemically reversible ferrocenyl oxidation signals followed by characteristic "stripping reduction peaks" showing evidence for oxidation-product electro-crystallization. Scanning electron microscopy confirmed spontaneous formation of crystalline oxidation products with three distinct morphologies for X = Cl^-, Br^-, I^-. Energy dispersive X-ray elemental analysis data show Fe:P ratios of 1:2.0, 1:2.1 and 1:2.1 for electro-crystallization products of complexes **2**, **3**, and **4**, respectively, indicating the presence of two $[PF_6]^-$ anions in the vicinity of the dioxidized complexes, and suggesting product formulae $[\mathbf{2}]^{2+}[PF_6]^-_2$, $[\mathbf{3}]^{2+}[PF_6]^-_2$ and $[\mathbf{4}]^{2+}[PF_6]^-_2$.

Introduction

Rationally designed, self-assembled supramolecular structures that create self-organized, functional materials are of fundamental interest for applications in catalysis,[1] gas storage or gas/molecule separations,[2] in nanotechnology,[3] and in electronic materials.[4] Organic molecules can self-assemble into well-ordered structures, but often with limited conductance. Conductivity can be influenced and improved by using coordination complexes in which metal centres are incorporated into a molecular backbone. Such structures self-assembled on insulating surfaces have been reported, for example, as highly conducting nano-ribbons.[3b] Solution-based rational self-assembly is a promising approach for the formation of microstructures with desired shapes.[5] In addition, incorporation of ferrocenyl or ferricenyl building blocks in the Fe(II) or the Fe(III) state, respectively, offer further material tuning opportunities and access to novel mixed-valence materials.[6]

Ferrocenyl functionalized coordination complexes are of particular interest due to the robust and switchable chemical nature of the ferrocene. Ferrocene also exhibits attractive electrochemical features:[7] fast electron-transfer rate,[8] low oxidation potential, and two easily accessible stable redox states (neutral ferrocene and oxidized ferricenium). Ferrocene-modified surfaces have been demonstrated to communicate efficiently *via* a lateral electron hopping process[9] and were recently highlighted for applications in charge storage components and in semiconductor-based memory devices with the bound ferrocene centre as the memory element.[10]

Ferrocene-based ligands with pyridine termini can be connected conveniently through an ethynyl linkage. The rigid rod character of the ethynyl linkage is known to facilitate electron delocalization in metal complexes.[11] We now report the reactions of the ferrocenyl-ethynylpyridine ligand (L) with the copper(I) halides (Cl^-, Br^- and I^-), in the presence of triphenylphosphine co-ligands, yielding square complexes $[L_2(CuCl)_2(PPh_3)_2]$ (**2**), $[L_2(CuBr)_2(PPh_3)_2]$ (**3**), and $[L_2(CuI)_2(PPh_3)_2]$ (**4**) *via* co-ordination driven self-assembly (see Scheme 1). Complete characterization of the square complexes using spectroscopic methods, X-ray crystallography and electrochemical techniques has been carried out. During electrochemical characterization of the complexes **2-4,** the electro-crystallization of

higher oxidation state products onto the electrode surface has been observed. The electro-crystallized products on a Pt disc working electrode surface were isolated and investigated by scanning electron microscopy (SEM) and energy dispersive X-ray (EDX) analysis for structural morphology and elemental composition. SEM data showed three distinct morphological arrangements (for X=Cl^-, Br^-, I^-) while the EDX suggested the formulae [**2**]$^{2+}$[PF_6]$^-_2$, [**3**]$^{2+}$[PF_6]$^-_2$ and [**4**]$^{2+}$[PF_6]$^-_2$ for the electro-crystallized products. In future, the design of materials of this type, in particular when based on mixed Fe(II/III) redox centres, could be of interest in novel mixed-valence electronic materials.[12]

Experimental

All syntheses were performed under a dry argon atmosphere using standard Schlenk or glovebox techniques. Solvents were pre-dried and distilled before use by standard procedures.[13] All chemicals and reagents, except where stated otherwise, were obtained commercially and used without further purification. The key starting material ethynylferrocene was synthesized by an adaptation of the literature method.[14] NMR spectra were recorded on a Bruker AM-400 spectrometer in $CDCl_3$. ^1H NMR spectra were referenced to solvent resonances and $^{31}P[^1H]$ NMR spectra were referenced to external trimethylphosphite. IR spectra were recorded in CH_2Cl_2 solution, in a NaCl cell, on a Nicolet-Impact 400D FT-IR spectrometer, and mass spectra obtained on a Kratos MS 890 spectrometer by the electron impact (EI) and fast atom bombardment (FAB) techniques. Microanalyses were performed in the Department of Chemistry, University of Bath, UK. Column chromatography was performed either on Kieselgel 60 (230 – 400 mesh) silica gel or celite.

Synthesis

Ferrocenyl-ethynylpyridine (1). Compound 1 was synthesized following a recently reported method.[15] IR (CH_2Cl_2) 2209 cm^{-1} ν(C≡C), 1454 cm^{-1} ν(C=N).^{1}H-NMR ($CDCl_3$): δ= 4.26 (s, 5H, H_{Cp}), 4.30 (pseudo-t, 2H, H_{Cp}), 4.54 (pseudo-t, 2H, H_{Cp}), 7.32 (d, *J* = 6.0 Hz, 4 H, $H_{β\text{-}pyr}$), 8.55 (d, *J* = 6.0 Hz, 4 H, $H_{α\text{-}pyr}$) ppm. FABMS: m/z 288 (M^+). Anal. Found: C, 71.78; H, 4.49%. Calc. $C_{17}H_{13}FeN$: C, 71.11; H, 4.56%.

$[L_2(CuCl)_2(PPh_3)_2]$ (**2**) with **(L = 1).** Ferrocenyl-ethynlpyridine **1** (80 mg, 0.28mmol) dissolved in 5 ml degassed dichloromethane (CH_2Cl_2) was added to a solution of CuCl (28mg, 0.28mmol) and triphenylphosphine (73mg, 0.28mmol) in 10 ml CH_2Cl_2**.** The mixture was allowed to stir for 24 h at room temperature. The crude product was obtained on removal of solvent under reduced pressure. The product was redissolved in CH_2Cl_2 and filtered through a plug of celite using hexane: CH_2Cl_2 (1:4 v/v). The filtrate was concentrated under reduced pressure to obtain orange micro crystals in 56% yield (102mg). IR (CH_2Cl_2) 2208 cm^{-1} ν(C≡C), 1488 cm^{-1} ν(C=N). ^{1}H-NMR (300.1 MHz, $CDCl_3$): δ(ppm) 4.26 (s, 10H, H_{Cp}), 4.33 (pseudo-t, 4H, H_{Cp}), 4.55 (pseudo-t, 4H, H_{Cp}), 7.40–7.90 (m, 34 H, P*Ph*$_3$, $H_{β\text{-}pyr}$) *δ* = 8.65 (d, *J* = 5.9 Hz, 4 H, $H_{α\text{-}pyr}$).^{31}P-NMR (121.53 MHz, $CDCl_3$): *δ* = 30.06 (s, P*Ph*$_3$) ppm. FAB-MS: m/z 1298 (M^+). $C_{70}H_{56}Cl_2Cu_2Fe_2N_2P_2$: Anal. Calcd: C, 64.83; H, 4.35%. Found: C, 64.88; H, 4.39 %.

$[L_2(CuBr)_2(PPh_3)_2]$ (**3**) with **(L=1)**. This compound was synthesized by following a procedure similar to that described above for **2** using **1** (80 mg, 0.28mmol), CuBr (40mg, 0.28mmol) and triphenylphosphine (73mg, 0.28mmol). The crude product, obtained by removal of solvent under reduced pressure, was re-dissolved in CH_2Cl_2 and filtered through a plug of celite using CH_2Cl_2. The filtrate was concentrated to obtain orange micro crystals in 63 % yield (122mg). IR (CH_2Cl_2) 2207cm^{-1} ν(C≡C), 1488cm^{-1} ν(C=N). ^{1}H-NMR (300.1 MHz, $CDCl_3$): δ (ppm) 4.26 (s, 10H, H_{Cp}), 4.33 (pseudo-t, 4H, H_{Cp}), 4.55 (pseudo-t, 4H, H_{Cp}), 7.39–7.85 (m, 34 H, P*Ph*$_3$, $H_{β\text{-}pyr}$) *δ* = 8.53 (d, *J* = 6.0 Hz, 4 H, $H_{α\text{-}pyr}$).^{31}P-

NMR (121.53 MHz, $CDCl_3$): δ = 30.06 (s, P*Ph*$_3$) ppm.FAB-MS: m/z 1387(M^+).$C_{70}H_{56}Br_2Cu_2Fe_2N_2P_2$: Anal. Calcd: C, 60.67; H, 4.07 %. Found: C, 60.71; H, 4.10 %.

[$L_2(CuI)_2(PPh_3)_2$] (**4**) with **(L = 1)**. This compound was synthesized by following a procedure similar to that described above for **2** using **1** (80 mg, 0.28mmol), CuI (53 mg, 0.28 mmol) and triphenylphosphine (73 mg, 0.28 mmol). The crude product obtained after removal of the solvent under reduced pressure was re-dissolved in CH_2Cl_2 and filtered through a pad of celite using CH_2Cl_2. The filtrate was concentrated to obtain orange micro crystals in 71 % yield (147mg). IR (CH_2Cl_2) 2206 cm^{-1} ν(C≡C), 1488 cm^{-1} ν(C=N). ^{1}H NMR (300.1 MHz, $CDCl_3$): δ(ppm)4.27 (s, 10H, H_{Cp}), 4.32 (pseudo-t, 4H, H_{Cp}), 4.55 (pseudo-t, 4H, H_{Cp}), 7.40–7.82 (m, 34 H, P*Ph*$_3$, $H_{\beta\text{-pyr}}$) δ = 8.42 (d, *J* = 6.1 Hz, 4 H, $H_{\alpha\text{-pyr}}$).^{31}P NMR (121.53 MHz, $CDCl_3$): δ = 30.09 (s, P*Ph*$_3$) ppm. FAB-MS: m/z: 1481. $C_{70}H_{56}Cu_2Fe_2I_2N_2P_2$: Anal. Calcd: C, 56.82; H, 3.81%. Found: C, 56.89; H, 3.87 %.

Scanning Electron Microscopy (SEM) and Energy Dispersive X-Ray Analysis (EDX). SEM images and EDX measurements were taken on a JEOL JSM 6480LV Scanning Electron Microscope using a BSE detector and an accelerating voltage of 15kV. SEM images were also taken on a JEOL JSM 6301F Field Emission Scanning Electron Microscope using an SEI detector and an accelerating voltage of 5kV. Solid samples were fixed to carbon tape that was mounted onto conductive SEM stubs. Electrodes were mounted on a holder and earthed to avoid charging of the surface.

Raman Spectroscopy. Raman spectra were recorded on a Renishaw inVia Raman Microscope using a solid state LASER with an excitation wavelength of 532nm and a power of 2.5mW. Samples were either mounted on a glass slide or on carbon tape for the solids and the spectra were taken using a 20x objective to focus on the crystals. Spectra for the electrodeposited product were taken directly from the electrode surface using the same objective.

Electrochemistry. Cyclic voltammetric studies were conducted in a glass cell under inert atmosphere (nitrogen) using a microAutolab III (Ecochemie, The Netherlands) under computer control using GPES software version 4.9. The electrochemical cell was 3 mm diameter platinum disc electrode, a Pt wire counter electrode, and KCl-saturated calomel electrode (Radiometer Ref 401) as reference electrode. All experiments were conducted in dichloroethane (DCE) with ca. 1 mM concentration for the complexes and using 0.1 M $[(n\text{-}C_4H_9)_4N][PF_6]$ as the supporting electrolyte.

Crystallography. Single-crystal X-ray diffraction experiments were performed at 150(2) K on either an Oxford Diffraction Gemini A Ultra CCD diffractometer (**2**, **4**) or an Nonius Kappa CCD diffractometer (**3**) using monochromatic Mo-K_α radiation (λ=0.71073 Å). For **2** and **4** the sample temperature was controlled using an Oxford Diffraction Cryojet apparatus; CrysAlis Pro was used for the collection of frames of data, indexing reflections and determining lattice parameters. For **3** the measurement temperature was controlled using an Oxford Cryostream device. Structures were solved by direct methods using SHELXS-86[16] and refined by full-matric least-squares, on F^2, using SHELX-97.[17] A multi-scan absorption correction was applied in all cases. Crystallographic data for all complexes studied can be found in Table 1. Complexes **2** and **3** were twinned, with **2** being treated as a racemic twin. In their crystalline forms both **2** and **3** contain molecules of CH_2Cl_2 in the crystal lattice; in **2** the CH_2Cl_2 is ordered and has full occupancy while in **3** there appear to be traces of hexane as well as CH_2Cl_2in the same lattice position though it was not possible to model this. The molecule of CH_2Cl_2 is itself disordered around a centre of inversion with an occupation factor of 30% in total. In the case of **3**, the cyclopentadienyl rings on the ferrocene moiety were disordered over two sites and the two sets of atomic positions were refined with occupancies summed to unity, while those in **2** showed rotational disorder that could not be modelled accurately. Overall, the

quality of the structures of **2** and **3** is poor but the connectivity of the atoms has been established unambiguously.

Table 1. Crystallographic data for **2-4**

Identification code	**2** (k12kcm48)Cl.CH_2Cl_2	**3** (h12kcm8) Br 0.6 CH_2Cl_2	**4** 185 I
Empirical formula	$C_{141}H_{114}Cl_6Cu_4Fe_4N_4P_4$	$C_{140.6}H_{115.2}Br_4Cl_{1.2}Cu_4Fe_4N_4P_4$	$C_{35}H_{28}CuFeINP$
Formula weight	2678.50	2824.38	739.84
Crystal system	Orthorhombic	Orthorhombic	Triclinic
Space group	$P2_12_12_1$ (No. 19)	$P2_12_12_1$ (No. 19)	P-1 (No. 2)
a (Å)	10.9453(2)	11.0168(3)	10.1206(4)
b (Å)	20.3553(4)	20.5385(6)	12.6511(6)
c (Å)	27.9598(7)	27.5647(8)	13.6628(7)
α(°)	90	90	104.106(4).
β(°)	90	90	106.750(4).
γ(°)	90	90	107.782(4).
V (Å^3)	6229.3(2)	6237.0(3)	1485.78(12)
T (K)	150(2)	150 (2)	150 (2)
Z	2	2	2
ρ_{calc}(Mgm^{-3})	1.428	1.504	1.654
μ(Mo-K_α) (mm^{-1})	1.354	2.530	2.322
F(000)	2740	2854	736
Crystal size (mm)	0.60 x 0.25 x 0.05	0.40 x 0.3 x 0.05	0.30 x 0.10 x 0.05
Theta range (°)	5.14 to 24.71	3.70 to 25.04	2.88 to 25.00
Reflections collected	32433	55648	14560
Independent refl'ns [R(int)]	10327 [0.0956]	10663 [0.0983]	7098 [0.0362]

Reflections observed (I>2σ(I))	7832	7267	5555
Data completeness	0.923	0.970	0.998
Max. and min. transmission	0.9354, 0.4973	0.8839, 0.3121	1.00, 0.744
Goodness-of-fit on F^2	1.02	1.043	1.024
Final R_1, wR_2 [I>2σ (I)]	0.0985, 0.2548	0.0729, 0.1573	0.0386, 0.0798
Final R_1, wR_2 (all data)	0.1276, 0.2793	0.1203, 0.1765	0.0579, 0.0889
Flack parameter	0.49(5)	0.30(3)	
Largest diff. peak, hole ($eÅ^3$)	1.963, -1.186	1.297, -0.597	0.943, -0.791

Results and Discussion

Synthesis and spectroscopic characterization. As reported recently, the cross-coupling reaction between ethynylferrocene[14] and 4-iodo-pyridine readily gave the known ferrocenyl-ethynylpyridine ligand **1** as brown powder in 81% yield.[15,18] For complexes **2-4** a 1:1:1 ratio of ligand **1**, CuX (X=Cl^-, Br^-, I^-) and triphenylphosphine were dissolved in dry dichloromethane under an argon atmosphere and allowed to stir for 24 h at room temperature. Neutral dimeric products formed where the pyridyl moiety of ligand **1** along with the co-ligand PPh_3 coordinate to same Cu in the $(CuX)_2$ rhomboid dimer (see Scheme 1). In the absence of PPh_3, under similar condition, the reactions gave rhomboid and cubic structures for CuCl, CuBr and CuI respectively.[12] All complexes (**2-4**) are stable to light and air at ambient temperature and were fully characterized by UV-vis, IR, NMR spectroscopy, FAB-mass spectrometry, as well as by satisfactory elemental analysis. Single crystal X-ray diffraction studies provided the full three-dimensional crystal structures, including the molecular dimensions of the dimeric complexes **2-4**.

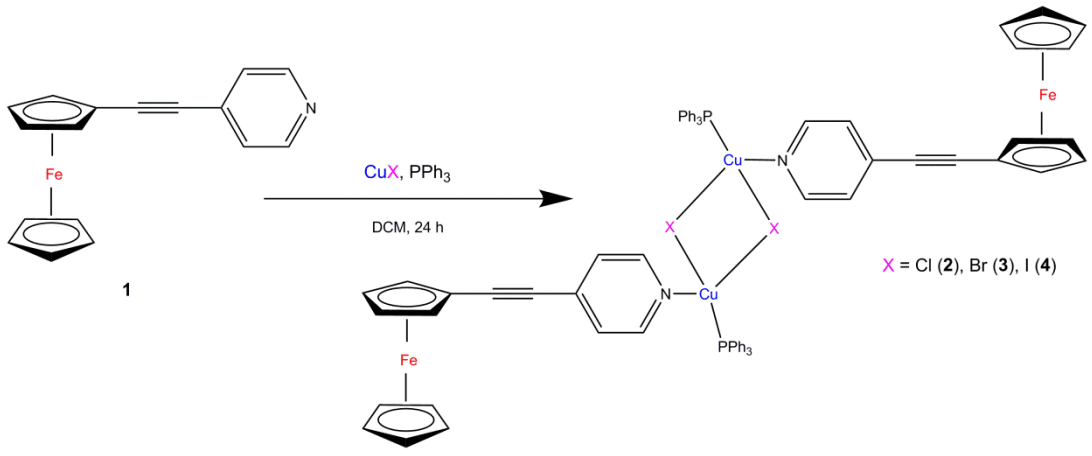

Scheme 1. Synthesis of neutral di-ferrocenyl-ethynylpyridinyl triphenylphosphine copper complexes **2-4**

The electronic absorption spectra of the complexes **2 - 4** were recorded in CH_2Cl_2 (Figure 1A, Table 2). Each compound displays two sets of absorption bands reminiscent of ferrocenyl-type species.[19] Bands with λ_{max} below 400 nm can be attributed to a π - π* transition associated with the organic group. A weak absorption band at ~450 nm is assigned to Fe^{II} *d-d* transition.[19a, 20]

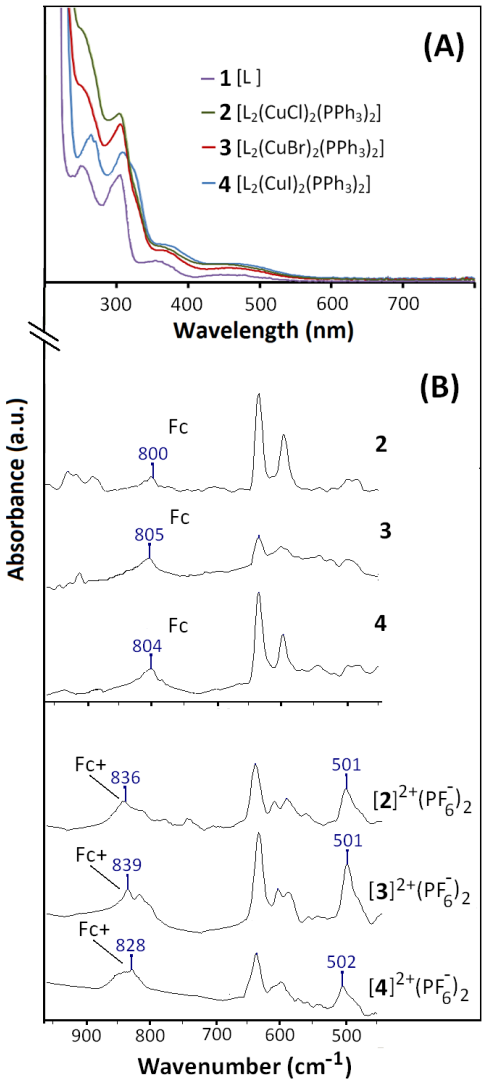

Figure 1. Panel (A): UV-vis spectra for ligand **1** and complexes **2-4** in dichloromethane. Panel (B): Raman vibrational spectra of complexes (**2-4**) and electro-crystallized products $[\mathbf{2}]^{2+}[PF_6]^-_2$, $[\mathbf{3}]^{2+}[PF_6]^-_2$ and $[\mathbf{4}]^{2+}[PF_6]^-_2$. Fc and Fc^+ in the figure stands for ferrrocene and ferricenium, respectively.

Table 2. UV-vis spectral data for **1** and complexes **2-4** in dichloromethane.

compound	**peak wavelength (λ_{max} / nm)**
1 [L]	255, 308, 350, 455
2 [$L_2(CuCl)_2(PPh_3)_2$]	258, 306, 383, 472
3 [$L_2(CuBr)_2(PPh_3)_2$]	262, 306, 384, 474
4 [$L_2(CuI)_2(PPh_3)_2$]	273, 311, 385, 475

The IR spectrum of the ligand **1** shows shifts in the bands on formation of complexes **2-4** (see Table 3). The pyridine vibration modes, like ν(pyridine ring) vibrations of **1** at 416 cm^{-1}, are positively shifted in complexes **2-4**. The variation in this band for complexes **2**-**4** is probably due to inductive effects of the halogens. Similarly, the pyridine ν(ring breathing) modes show positive shift on complex formation and further minor changes due to halogen effect.[21] Also the $\nu Cp_{(Fc)}$ ring vibration exhibits a positive shift in the complexes **2-4**. The ν(FeCp) vibration shows a negative shift when going from ligand **1** to complexes **2-4,** however, among the complexes there is no significant variation in the ν(FeCp) band. The reason for this could be the long distance of the FeCp from the electronegative halogens.[22] Similarly, a single sharp band for $\nu_{(C\equiv C)}$ around 2210 cm^{-1}, characteristic of ethynylferrocenyls[11c, 23] bonded to aromatic and hetero-aromatic spacer groups and perpendicular C−H bending vibration at 821 cm^{-1} for ferrocene,[24] are observed in ligand **1** which shows minor change in complexes **2-4,** again due to long distance from the coordination centre.

Table 3. Selected IR vibrational frequencies (cm^{-1}) of **1** and complexes (**2-4**).

1	**2**	**3**	**4**	Assignment
416	438	428	418	Ring (Py)
484	472	472	472	ν(FeCp)
821	822	823	823	C-H (Fc)
1106	1120	1119	1120	Cp_{Fc} breathing
1170	1185	1188	1189	Ring breathing (Py)
2210	2207	2206	2005	ν(C≡C)

Py=Pyridinyl

Trends similar to those in the IR data were observed in the Raman bands for **1** upon coordination to Cu-X (X = Cl^-, Br^-, I^-) as shown in Table 4. The Cu–N and Cu–X stretching vibrations were observed at ~296cm^{-1} and ~326 cm^{-1}, respectively, similar to some Cu-pyridine complexes reported previously.[25] The CN stretching vibration in the pyridine ring of the ligand was observed at 1592 cm^{-1}, exhibiting a positive shift upon coordination; similarly, the CNC bending vibrations of pyridine ring show a positive shift on complex formation.[21] The ethynyl C≡C vibration band and the ferrocenyl ring breathing modes are observed at 2209 cm^{-1} and 1106 cm^{-1}, respectively. There is only minor shift in these two bands upon complex formation, due to the relatively large distance between the terminal ethynyferrocenes and the Cu-coordination site.

Table 4. Selected solid state Raman vibrational frequencies (cm^{-1}) of **1**, complexes **2-4** and electro-crystallized products $[\mathbf{2}]^{2+}[PF_6]^-_2$, $[\mathbf{3}]^{2+}[PF_6]^-_2$ and $[\mathbf{4}]^{2+}[PF_6]^-_2$.

1	2	3	4	$[2]^{2+}[PF_6]^-_2$	$[3]^{2+}[PF_6]^-_2$	$[4]^{2+}[PF_6]^-_2$	Assignment
-	296	296	296	288	288	290	Cu-X [X=Cl(**2**),Br(**3**), I(**4**)]
-	328	328	328	313	315	318	Cu-N
1592	1597	1599	1597	1615	1611	1603	CN stretching (Py)
989	1006	1013	1006	1031	1025	1014	CNC bending (Py)
1173	1172	1173	1172	1177	1177	1176	Ring breathing (Py)
1106	1108	1108	1108	1112	1110	1110	Cp_{Fc} breathing
2209	2207	2203	2207	~2217[a]	~2215[a]	~2216[a]	ν(C≡C)
	800	806	804	836	839	828	C-H bending (Fc)
-	-	-	-	499	499	501	$\nu(PF_6^-)$

[a] broad split peak

Most Raman bands for the electro-crystallized products $[\mathbf{2}]^{2+}[PF_6]^-_2$, $[\mathbf{3}]^{2+}[PF_6]^-_2$ and $[\mathbf{4}]^{2+}[PF_6]^-_2$ exhibit only minute shifts when compared to those of the neutral parent complexes **2**, **3** and **4** (Table 4). The Fc breathing modes exhibit a positive shift while the Cu-N and Cu-X vibrations show consequential contraction or negative shifts in the fully oxidized species $[\mathbf{2}]^{2+}[PF_6]^-_2$, $[\mathbf{3}]^{2+}[PF_6]^-_2$ and $[\mathbf{4}]^{2+}[PF_6]^-_2$. The CN stretching vibration, CNC bending vibration and the pyridine ring breathing mode also show positive shifts in the Raman spectra of the oxidized species. A broad split peak is observed, ranging from 2210 to 2230 cm^{-1} for the C≡C vibration. Broad split Raman peaks have been reported for oxidation products in other systems.[26] As Raman spectroscopy is a complimentary technique to IR spectroscopy most of the IR bands also appear in Raman spectra with minor variations. We note an interesting Raman band at ~800 cm^{-1} for complexes **2-4** (ferrocene C-H bending) being converted to ~830 cm^{-1} in $[\mathbf{2}]^{2+}[PF_6]^-_2$ to $[\mathbf{4}]^{2+}[PF_6]^-_2$ (ferricenium C-H) with little change in intensity. Jiao *et. al*.,[24b] Nemykin *et. al*.[24a] and others[24c] have reported analogous shift in IR spectroscopy for perpendicular C-H bending vibration as the benchmark for conversion of ferrocene to ferricenium ion.[24b] A peak at

around 500 cm^{-1} is observed for the $[PF_6]^-$ counter ion[24] in all oxidized products $[\mathbf{2}]^{2+}[PF_6]^-_2$, $[\mathbf{3}]^{2+}[PF_6]^-_2$ and $[\mathbf{4}]^{2+}[PF_6]^-_2$ (Figure 1).

The ^1H NMR spectra showed a pattern of singlet and (pseudo) triplet *i.e.*, overlapping *dd* signals at ~4ppm for the unsubstituted C_5H_5 and substituted C_5H_4 ferrocenyl Cp protons, respectively.[28] Pyridinyl (C_5H_4N) proton and P*Ph*$_3$-H signals were observed in the 7 - 9 ppm region as doublets and complex multiplets as expected.[29] The pyridinyl-Hs_β were often overlapped with the P*Ph*$_3$ H-atoms as they appear in the same region in the spectra. Some relaxation in the pyridinyl-H_α of the ligand was seen upon complex formation. Further, among the complexes **2-4** there are minor but gradual upfield shift in the pyridinyl-H_α which can be attributed to the decreasing deshielding (inductive) effect of the halogens along the series (Cl-, Br-, I-). Mass spectra (+ve FAB) displayed the presence of molecular ions with characteristic fragmentation patterns for the complexes. The structures of the complexes **2** - **4** were further confirmed by X-ray crystallography.

Structural characterization. The parent compound, Fc-C≡C-py **1** forms adducts of the type $[(\mathbf{1})Cu(X)(PPh_3)]_2$ with CuX, X = Cl^- (**2**), Br^- (**3**), I^- (**4**). This dimeric or square arrangement is well established, and the structures follow that of the prototype $[(py)(PPh_3)CuX]_2$ (py = C_5H_5N) determined over two decades ago.[30] Compounds **2** and **3** are *iso*-structural (see Figure 2) but lack the symmetry inherent in **4** (see Figure 3), although they qualitatively adopt the same structure. In all three cases, there is *trans* arrangement of pairs of phosphines and pyridines around a central Cu_2X_2 ring, enforced by symmetry in the case of **4** (due to an inversion centre at the heart of the Cu_2I_2 ring). The geometry about copper in all cases is a distorted tetrahedron, with bond angles in the range 103.4(4) – 117.95(15) (**2**), 105.9(4) – 116.35(15) (**3**), 100.50(8) – 115.47(3)^o (**4**); the Cu-X, Cu-P and Cu-N bond lengths are unexceptional (see Table 5) and are similar to the parent $[(py)(Ph_3P)CuX]_2$ systems.[30] The Cu_2X_2 ring geometries are also similar to those in $[(py)(Ph_3P)CuX]_2$, save for **4** where

the angle at iodine is wider [70.405(16) *vs*. 67.13(7), 67.55(9)°] and the angle at copper narrower [109.595(16) *vs*. 112. 66(6)°].

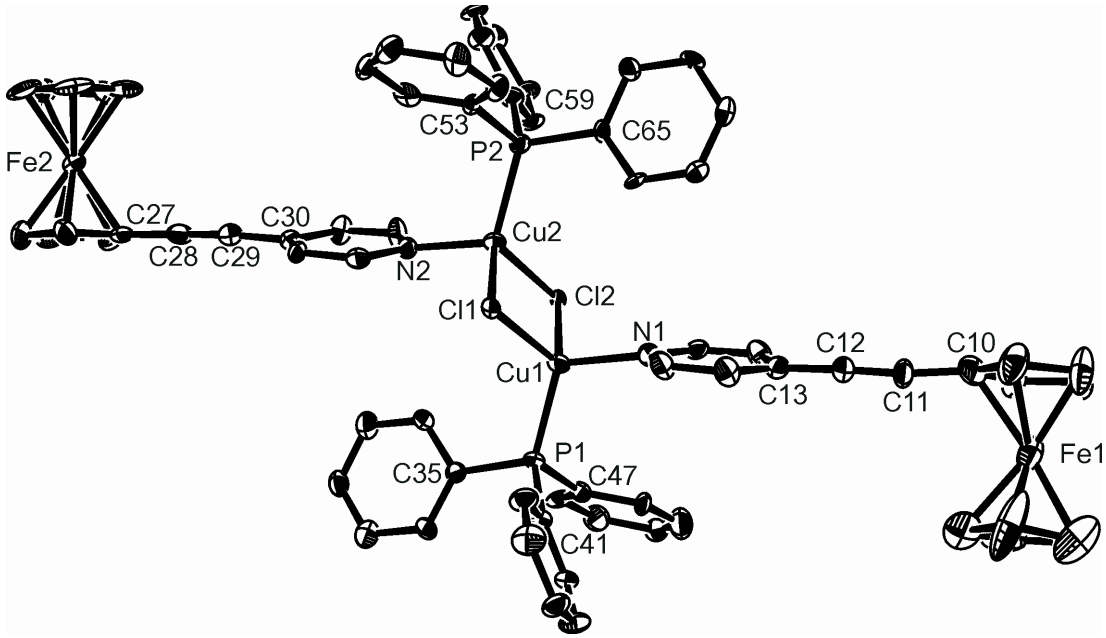

Figure 2. The structure of **2.**CH_2Cl_2 showing the asymmetric unit and the labelling scheme used in the text; only the α-carbons of the phenyl rings have been labelled for clarity. Thermal ellipsoids are at the 30% level. Selected additional geometric data for **2** and **3**: **2**: Fe(1)-C(1,5) ring centroid 1.652(11), Fe(1)-C(6,10) ring centroid 1.651(7) Å, N(1)-Cu(1)-P(1) 113.0(4), N(1)-Cu(1)-Cl(1) 103.4(4),N(1)-Cu(1)-Cl(2) 105.4(4), P(1)-Cu(1)-Cl(1) 116.76(16),P(1)-Cu(1)-Cl(2) 111.16(16), Cl(1)-Cu(1)-Cl(2) 106.27(13), Cu(1)-Cl(1)-Cu(2) 74.04(13), Cu(1)-Cl(2)-Cu(2) 73.61(11)°; **3**: Fe(1)-C(1,5) ring centroid 1.536(13), Fe(1)-C(6,10) ring centroid 1.602(8) Å, N(1)-Cu(1)-P(1) 112.7(4), N(1)-Cu(1)-Br(1) 103.9(4), N(1)-Cu(1)-Br(2) 105.9(4), P(1)-Cu(1)-Br(1) 116.35(15), P(1)-Cu(1)-Br(2) 109.72(15), Br(2)-Cu(1)-Br(1) 107.65(9), Cu(2)-Br(1)-Cu(1) 71.85(7), Cu(2)-Br(2)-Cu(1) 72.44(7) °.

In contrast to the geometry in compound **1** the C_5H_4 and NC_5H_4 rings in **2-4** are twisted with respect to each other; for **4**, the angle between C(7)-C(10) and C(13)-N(1) planes is 22.44(14)° and the loss of conjugation that results is manifest in a lengthening of the C-C(py) bond from 1.378(4) (**1**) to 1.432(4) Å (**4**). However, the relationship between the co-planarity of the C_5H_4 and NC_5H_4 rings and the extent of delocalization along the $(C_5H_4)C{\equiv}C(C_5H_4N)$ chain is less than clear cut, as in **3** the analogous twist angles [*e.g*. C(5)-C(10) / C(13)-N(1)] are smaller [7.82(1.33), 11.84(0.73) °] though the C-C(py) bond is longer than in **4** [1.455(18)], 1.453(19) Å], while for **2** the reverse is true [twist angles: 18.33(0.87), 15.94(0.83); C-C(py): 1.38 (2), 1.35(2) Å]. In addition, neither the C≡C nor the

FcC-C(≡C) bond lengths alter significantly or systematically along the series within experimental error. This suggests that ligand coordination to copper impacts on the pyridine, but not on the alkynylferrocene moiety. It seems likely, therefore, that packing effects are as important as electronic effects in the overall spatial arrangement of ligands around copper.

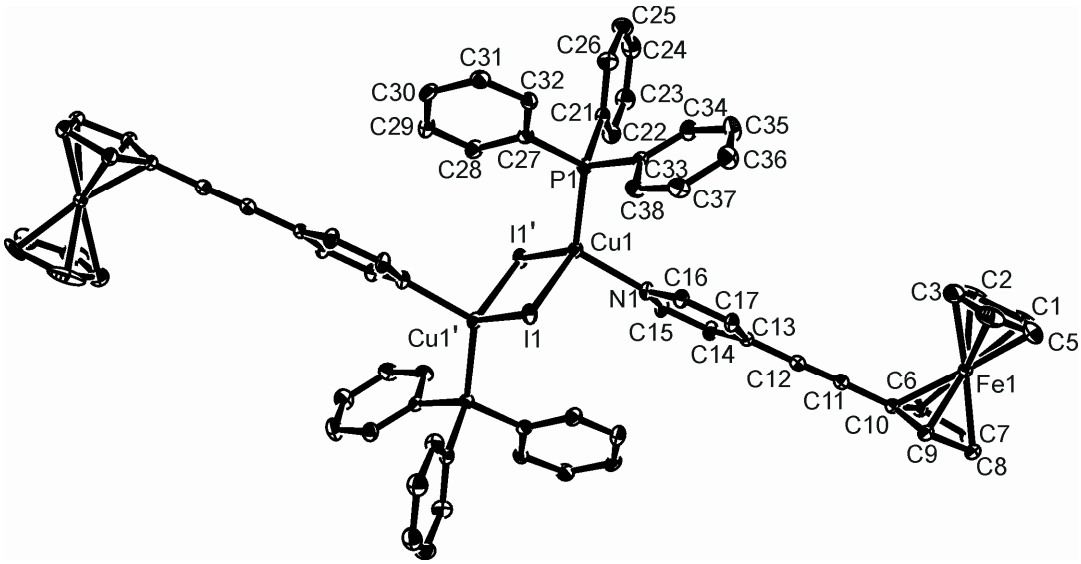

Figure 3. The structure of **4** showing the asymmetric unit and the labelling scheme used in the text; thermal ellipsoids are at the 30% level. Selected geometric data: Fe(1)-C(1,5) ring centroid 1.658(2), Fe(1)-C(6,10) ring centroid 1.643(2), N(1)-Cu(1)-P(1) 114.62(8), N(1)-Cu(1)-I(1') 106.62(8), P(1)-Cu(1)-I(1') 115.47(3), N(1)-Cu(1)-I(1) 100.50(8), P(1)-Cu(1)-I(1) 108.95(3), I(1)-Cu(1)-I(1') 109.595(16), Cu(1)-I(1)-Cu(1') 70.405(16); additional data are given in Table 5. Symmetry operation: *.1-x,-y,1-z*.

Table 5.Comparative data from crystallography: Fc-C≡C-C and N:→Cu geometric data for **2 – 4**

	C≡C (Å)	Fe-C(≡C) (Å)	(C≡)C-C(py)(Å)	∠C-C≡C-C (°)	Cu-X (Å) [a]	P:→Cu (Å)	N:→Cu (Å)
1 [b]	1.209(4)	1.415(4)	1.378(4)	178.5(3), 179.3(3)			
2	1.25(2) 1.22(3)	1.41(2) 1.40(3)	1.38(2) 1.47(2)	168(2), 177(2) 178(2), 175.4(19)	2.442(3) 2.463(5) 2.433(4) 2.479(4)	2.193(4) 2.195(4)	2.061(13) 2.047(12)
3	1.207(17) 1.172(15)	1.444(18) 1.419(16)	1.455(16) 1.453(17)	177.1(18), 176.7(14) 178.2(13), 177.5(14)	2.5011(17) 2.522(2) 2.4976(18) 2.5127(16)	2.208(3) 2.211(3)	2.045(19) 2.041(9)
4	1.200(4)	1.430(4)	1.432(4)	178.5(4), 176.7(4)	2.6405(5) 2.6861(5)	2.2348(10)	2.071(3)
$[(py)(Ph_3P)CuCl]_2$ [c]					2.409(3), 2.381(3)	2.189(2)	2.083(7)
$[(py)(Ph_3P)CuBr]_2$ [c]					2.538(2), 2.507(2)	2.209(3)	2.053(9)
$[(py)(Ph_3P)CuI]_2$ [c]					2.692(3), 2.677(3)	2.240(3)	2.048(7)

[a]X = appropriate halogen, specifically Cl (**2**), Br (**3**), I (**4**) b = ref [15] c= ref.[30]

Electrochemistry. Redox properties of **1-4** were investigated using cyclic voltammetry in dichloroethane, and with redox potentials reported versus saturated calomel electrode (SCE). A summary of data is collected in Table 6. Cyclic voltammograms were obtained in a potential window typical for ferrocene redox systems and with a range of scan rates (50-1000 mVs^{-1}) for *ca.* 1mM solutions of **1-4** in dichloroethane (DCE) with 0.1 M [*n*-Bu_4N]PF_6 as supporting electrolyte and at room temperature. The voltammograms for **1** showed a single redox process with midpoint potentials ($E_{1/2}$) at 692 mV [here $E_{1/2}$ = 0.5($E_{p,ox}$ + $E_{p,red}$)] (not shown). Voltammograms for complexes **2-4** are consistent with a ferrocene-based redox process with broadened oxidation and back-reduction peaks. Broad redox peaks have been reported previously for weakly interacting ferrocenes in multi-ferrocenyl complexes[31] and in part this mechanism could be active here. However, additional peak shape complexity here is due to electro-crystallization of product (*vide infra*). The midpoint potentials $E_{1/2}$ for compounds **2-4** ranged from 534 mV to 613 mV. These values are lower compared to that for compound **1** and the lower $E_{1/2}$ values for ferrocenyl co-ordination complexes compared to the ferrocenyl ligand could be attributed to the electrostatic stabilization between the multi-ferricenium cation and the counter anionic moieties as observed earlier in analogous systems.[32] $E_{1/2}$ values for **1-4** are more positive when compared to standard ferrocene under same conditions ($E_{1/2}$= 527mV *vs*. SCE) which is expected for electron-withdrawing ethynylferrocene complexes.[20b, 33]

Interestingly, at lower scan rates the broad oxidation peak were followed by a very narrow "stripping" back-reduction peak, particularly visible for complexes **2** and **3** and at the lowest scan rates[34] (see Figure 4). The sharp stripping reduction peak is indicative of electro-crystallization of the oxidation product followed by cathodic "stripping".[35]

Table 6. Electrochemical potential data in mV vs. SCE for complexes **1**-**4** obtained from cyclic voltammograms at a 3 mm diameter platinum electrode with scan rate 100 mVs^{-1} in DCE solution containing 0.1 M [n-Bu_4N^+][PF_6^-], at 25±2°C, errors estimated.

Complex	$E_{p,ox}$ ±5 (mV)	$E_{p,red}$ ±5 (mV)	$\Delta E = (E_{p,ox}-E_{p,red})$ ±5 (mV)	$E_{½}= ½(E_{p,ox}+E_{p,red})$ ±5 (mV)
1	786	599	187	692
2	638	500	138	569
3	627	442	185	534
4	701	526	175	613

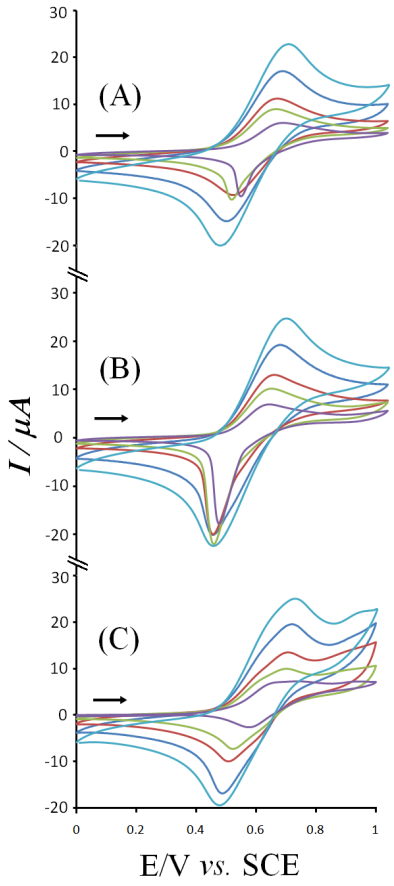

Figure 4. Cyclic voltammograms(scan rates 50, 100, 200, 500 and 1000mVs^{-1}) obtained at a 3 mm diameter platinum electrode for complexes **2,3** & **4** as (A), (B) & (C)respectively, in DCE with 0.1 M [*n*-Bu_4N]PF_6 as supporting electrolyte at 25 °C± 2.

In order to attempt isolation of the oxidation product, a setup with 3 mm Pt disc working electrode and Pt wire collector electrode immersed in *ca*. 1mM solution of complex **2** in DCE with 0.1 M [*n*-Bu_4N^+][PF_6^-] as supporting electrolyte was prepared and the potential was held constant for deposition at0.9 V vs. SCE for 300 seconds. The colour of the solution became darker with time and the formation of a deposit at the electrode surface was observed by in situ optical microscopy. The electrode was removed from the solution with potential applied, washed with a few drops of DCE, and the product remaining on the electrode surface was dried under vacuum for 12 h. The morphology of the crystalline deposits were analyzed by scanning electron microscopy (SEM). The approximate elemental composition was confirmed by energy-dispersive X-ray (EDX) analysis. Raman analysis for the electro-crystallized products was also performed (*vide supra*). A similar procedure was employed for the oxidation products of complexes **3** and **4.**

SEM analysis confirmed the spontaneous formation of the crystalline oxidation products on the electrode surface (see Figure 5). Copper compounds are widely used as catalyst and electrodeposited Cu-based microstructures are of interest for potential applications in catalysis.[36] SEM images of the electro-crystallized product of complex **2** show leaf-like growth of the crystals on the electrode surface. Similarly, for electro-crystallized products of complex **3**, the SEM images show leaf-like morphology but the leaf are bigger in size and more angular in shape compared to electro-crystallization product of **2**. For electro-crystallized product of complex **4** the SEM images show cabbage-like morphology. The three distinct morphologies observed for the electro-crystallized products (X = Cl^-, Br^-, I^-) indicate the potential of the system for controlling the shape of the electro-deposited microstructures. The shapes of the

electrodeposited micro structures could be important for enhancing the catalytic activity and selectivity of metallic catalysts.[36d]

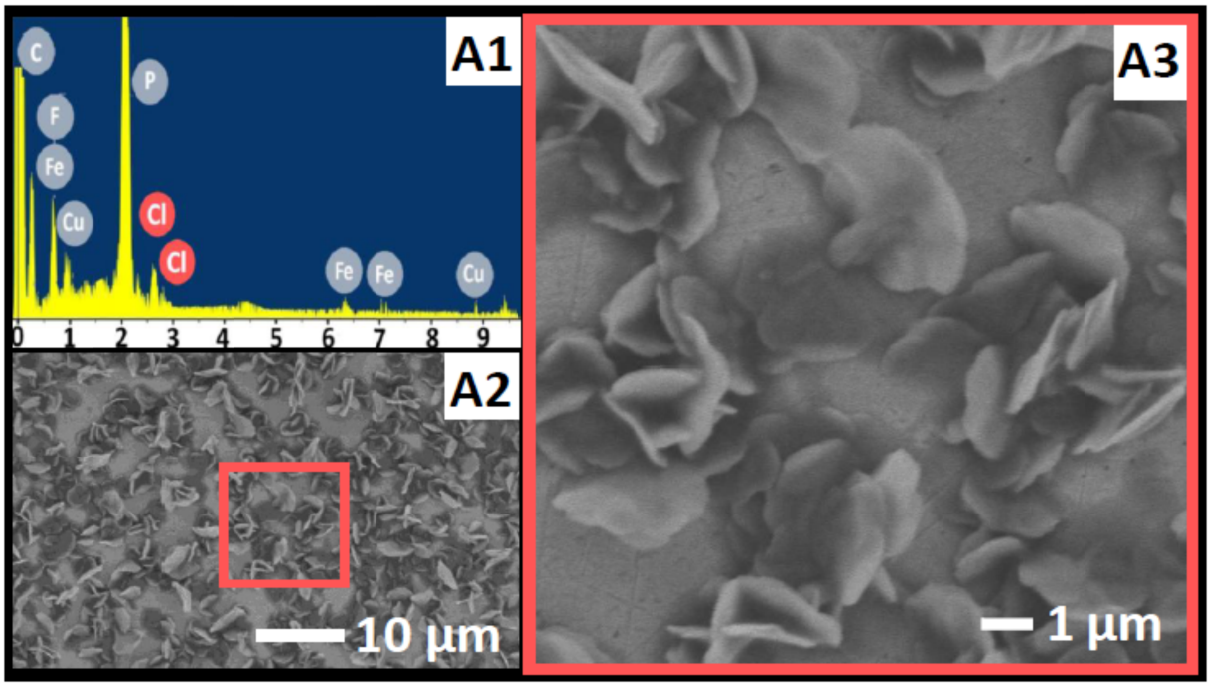

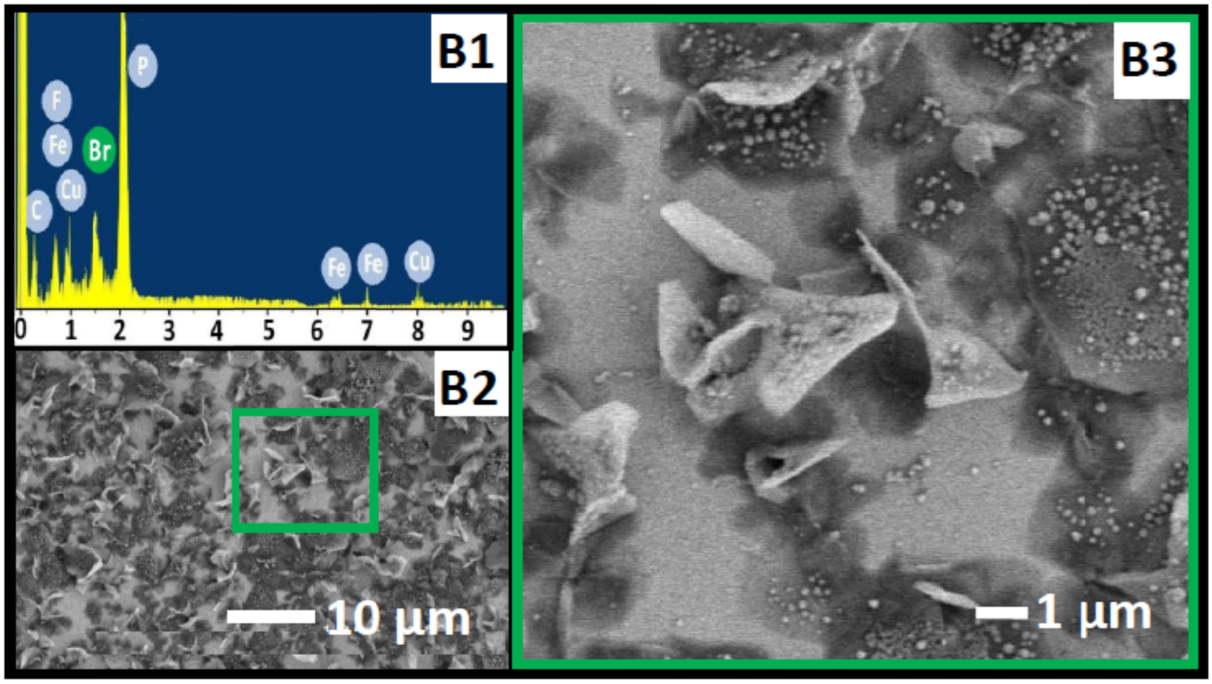

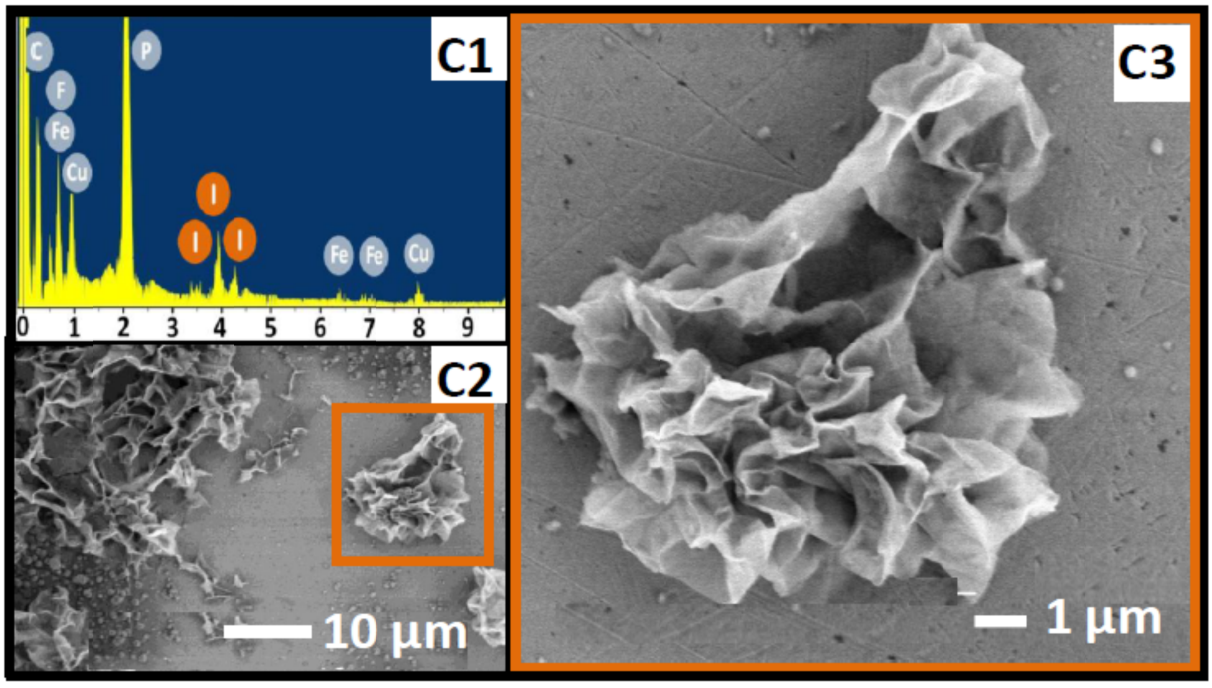

Figure 5. SEM images of electro-crystallized products from 1 mM solution in DCE with 0.1M [*n*-Bu_4N^+]PF_6^- electrodeposited for 300 sec at +0.9 V. Panels : (A1) (B1) and (C1) are the EDX spectra while; (A2), (B2) & (C2) show low magnification and (A3), (B3) and (C3) show high-magnification SEM images for electro-crystallized products [**2**]$^{2+}$[PF_6]$^-$, [**3**]$^{2+}$[PF_6]$^-_2$ and [**4**]$^{2+}$[PF_6]$^-_2$, respectively.

The electrodeposition was conducted at a potential much higher than the redox potential of the complexes. Thus, the electro-crystallized products are believed to be fully oxidized (two-electron oxidized), and associated with two [PF_6]$^-$ anions from the supporting electrolyte. Approximate EDX analysis supports this assumption showing the Fe:Cu, Cu:Cl, and Fe:P ratios 1:1.2, 1:1, and 1:2, respectively, in broad agreement (within experimental error of EDX) with the proposed dimeric dicationic product complex [**2**$^{2+}$][PF_6]$^-_2$ (see Table 7). Similarly, for electro-crystallized products of complex **3**, the EDX data suggest Fe:Cu, Cu:Br, and Fe:P ratios 1:1.4, 1:1, and 1:2.1, respectively, in broad agreement with the proposed dimeric dicationic product complex [**3**$^{2+}$][PF_6]$^-_2$. For electro-crystallized product of complex **4** the EDX data suggest Fe:Cu, Cu:Cl, and Fe:P ratios of 1:1.2, 1:1.0, and 1:2.1, respectively, in agreement with the proposed dimeric dicationic product complex [**4**$^{2+}$][PF_6]$^-_2$.

Table 7. EDX compositional data summarized for electro-crystallized products [**2**]^2[PF_6]$^-_2$, [**3**]$^{2+}$ [PF_6]$^-_2$ and [**4**]$^{2+}$[PF_6]$^-_2$. Key elemental ratios are given**.**

	Fe : Cu	Cu : X (X=Cl, Br & I)	Fe : P	P : F
[**2**]$^{2+}$[PF_6]$^-_2$ or [$L_2(CuCl)_2(PPh_3)_2$]$^{2+}$[PF_6]$^-_2$	1:1.2	1:1.0	1:2.0	1:3.6
[**3**]$^{2+}$[PF_6]$^-_2$or [$L_2(CuBr)_2(PPh_3)_2$]$^{2+}$[PF_6]$^-_2$	1:1.4	1:1.0	1:2.1	1:2.8
[**4**]$^{2+}$[PF_6]$^-_2$ or [$L_2(CuI)_2(PPh_3)_2$]$^{2+}$[PF_6]$^-_2$	1:1.2	1:1.0	1:2.1	1:3.0

In the future a full study including crystallography of the oxidation products is desirable. In all the above electro-crystallizations the dominating products are consistently doubly-oxidized with $[PF_6]^-$ counter anions co-crystallized during the complex formation. Co-crystallization of donor-acceptor components in a crystal lattice as mixed stacks has been recently reported to lead to intra-molecular charge transfer properties.[37] The convenient production and isolation of oxidized materials reported here could be of interest for novel ferroic materials,[38] whereas design of complex shapes from simple components with a high level of control over morphology holds promise for future applications in optics and catalysis.[39]

Conclusions

A simple and convenient synthesis has been developed for a series of neutral di-ferrocenyl-ethynylpyridinyl triphenylphosphine copper halide complexes. The neutral di-nuclear complexes can be oxidized under mild conditions with formation of the fully oxidized electro-crystallization products. Electro-deposition of the oxidation products gave a new series of dicationic di-ferricenyl-ethynylpyridinyl copper halide materials. The inherent structural features common to the reaction products are based on aromatic and ethyne units as well as the rhomboid bimetallic centres that potentially provide high electron-mobility. These crystalline materials with fully or partially occupied ferrocene electronic band structure will be of interest in future electronic materials and in optical components.[40] The incorporation of $[PF_6]^-$ into the structure can be considered as "structurally well-defined" doping with implications for photo-excitation and electronic conductivity (with IVCT bands in the NIR range).[41] A combination of mobile electrons and structural rearrangements are possible in these

novel materials that could offer an entry into a new class of multi-ferroics[38b, 42] or mixed electronic/ionic conductors.[43]

Acknowledgements

MSK acknowledges Sultan Qaboos University for a Research Grant: IG/SCI/CHEM/13/01 and for a research leave while HHS and RAAl-B acknowledge Sultan Qaboos University, Oman for PhD scholarships. We are grateful to the British Council for a PMI-2 Grant (GS 216) that has supported MSK, MKAl-S, HHS, KCM and PRR. PRR gratefully acknowledges support from the EPSRC through the award of a Senior Fellowship (EPSRC EP/D072859/1) and CHW for a project studentship (EPSRC EP/F021151/1). This work was conducted as part of the Project: ORG/EI/13/010 submitted to The Research Council (TRC), Oman.

Supporting Information

†Electronic Supplementary Information (ESI) available: Crystallographic data for the structural analysis (in CIF format) have been deposited with the Cambridge Crystallographic Data Centre, CCDC nos. 1000004-1000006 for **2** - **4**, respectively. Copies of this information may be obtained from the Director, CCDC, 12 Union Road, Cambridge, CB2 1EZ, UK (Fax: +44-1233-336033; e-mail: deposit@ccdc.cam.ac.uk or www.ccdc.cam.ac.uk). For ESI and crystallographic data in CIF or other electronic format see DOI: 10.1039/xx000000x/

References

1. G. Givaja, P. Amo-Ochoa, C. J. Gomez-Garcia and F. Zamora, *Chem. Soc. Rev.*, 2012, **41**, 115-147.

2. D. Tanaka, K. Nakagawa, M. Higuchi, S. Horike, Y. Kubota, T. C. Kobayashi, M. Takata and S. Kitagawa, *Angew. Chem. Int. Ed.*, 2008, **47**, 3914-3918.

3. a) K. Ariga, H. Ito, J. P. Hill and H. Tsukube, *Chem. Soc. Rev.*, 2012, **41**, 5800-5835; b) L. Welte, A. Calzolari, R. Di Felice, F. Zamora and J. Gomez-Herrero, *Nat Nano*, 2010, **5**, 110-115.

4. a) A. P. H. J. Schenning and E. W. Meijer, *Chem. Commun.*, 2005, 3245-3258; b) J. Kang, J. A. Nelson, M. Lu, B. Xie, Z. Peng and D. R. Powell, *Inorg. Chem.*, 2004, **43**, 6408-6413.

5. a) J. E. M. Lewis, C. John McAdam, M. G. Gardiner and J. D. Crowley, *Chem. Commun.*, 2013, **49**, 3398-3400; b) P. A. Rupar, L. Chabanne, M. A. Winnik and I. Manners, *Science*, 2012, **337**, 559-562; c) M. D. Ward and P. R. Raithby, *Chem. Soc. Rev.*, 2013, **42**, 1619-1636.

6. a) A. K. Diallo, C. Absalon, J. Ruiz and D. Astruc, *J. Am. Chem. Soc.*, 2011, **133**, 629; b) S.-H. Wu, J.-J. Shen, J. Yao and Y.-W. Zhong, *Chemistry – An Asian Journal*, 2013, **8**, 138-147.

7. A. L. Eckerman, D. J. Feld, J. A. Shaw and T. J. Meade, *Coord. Chem. Rev.*, 2010, **254**, 1769-1802; R. Horikoshi and T. Mochida, *Eur. J. Inorg. Chem*., 2010, **34**, 5355-5371.

8. N. Fietkau, A. D. Clegg, R. G. Evans, C. Villagran, C. Hardacre and R. G. Compton, *ChemPhysChem*, 2006, **7**, 1041-1045.

9. a) S.-H. Hsu, D. N. Reinhoudt, J. Huskens and A. H. Velders, *J. Mater. Chem.*, 2011, **21**, 2428-2444; b) S. Eyley, S. Shariki, S. E. Dale, S. Bending, F. Marken and W. Thielemans, *Langmuir*, 2012, **28**, 6514-6519.

10. B. Fabre, *Acc. Chem. Res.*, 2010, **43**, 1509.

11. a) M. S. Khan, M. K. Al-Suti, H. H. Shah, S. Al-Humaimi, F. R. Al-Battashi, J. K. Bjernemose, L. Male, P. R. Raithby, N. Zhang, A. Kohler and J. E. Warren, *Dalton Trans.*, 2011, **40**, 10174-10183; b) A. Kohler, A. L. T. Khan, J. S. Wilson, C. Dosche, M. K. Al-Suti, H. H. Shah and M. S. Khan, *J. Chem. Phys*, 2012, **136**, 094905-094908; c) H. H. Shah, R. A. Al-Balushi, M. K. Al-Suti, M. S. Khan, C. H. Woodall, K. C. Molloy, P. R. Raithby, T. P. Robinson, S. E. C. Dale and F. Marken, *Inorg.*

Chem., 2013, **52**, 4898-4908; d) J. S. Wilson, A. S. Dhoot, A. J. A. B. Seeley, M. S. Khan, A. Köhler and R. H. Friend, *Nature*, 2001, **413**, 828; e) L. Sudha Devi, M. K. Al-Suti, N. Zhang, S. J. Teat, L. Male, H. A. Sparkes, P. R. Raithby, M. S. Khan and A. Köhler, *Macromol.*, 2009, **42**, 1131-1141; f) P. Li, B. Ahrens, N. Feeder, P. R. Raithby, S. J. Teat and M. S. Khan, *Dalton Trans.*, 2005, 874-883; g) M. S. Khan, M. R. A. Al-Mandhary, M. K. Al-Suti, F. R. Al-Battashi, S. Al-Saadi, B. Ahrens, J. K. Bjernemose, M. F. Mahon, P. R. Raithby, M. Younus, N. Chawdhury, A. Kohler, E. A. Marseglia, E. Tedesco, N. Feeder and S. J. Teat, *Dalton Trans.*, 2004, 2377-2385; h) J. S. Wilson, R. J. Wilson, R. H. Friend, A. Köhler, M. K. Al-Suti, M. R. A. Al-Mandhary and M. S. Khan, *Physical Review B*, 2003, **67**, 125206; i) J. S. Wilson, A. S. Dhoot, A. J. A. B. Seeley, M. S. Khan, A. Kohler and R. H. Friend, *Nature*, 2001, **413**, 828-831; j) J. S. Wilson, N. Chawdhury, M. R. A. Al-Mandhary, M. Younus, M. S. Khan, P. R. Raithby, A. Köhler and R. H. Friend, *J. Am. Chem. Soc.*, 2001, **123**, 9412-9417.

12. O. Gidron, Y. Diskin-Posner and M. Bendikov, *Chem. Eur. J.*, 2013, **19**, 13140-12150; Y. Ochi, M. Suzuki, T. Imaka, M. Murata, H. Nishihara, Y. Einaga and K. Yamamoto, *J. Am. Chem. Soc*., 2010, **132**, 5061-5069.
13. W. L. F. Armarego, in *Purification of Laboratory Chemicals (Sixth Edition)*, Butterworth-Heinemann, Oxford, 6th Edition, 2009, p. xv.
14. S.-J. Luo, Y.-H. Liu, C.-M. Liu, Y.-M. Liang and Y.-X. Ma, *Synth. Commun.*, 2000, **30**, 1569-1572.
15. H. H. Shah, R. A. Al-Balushi, M. K. Al-Suti, M. S. Khan, C. H. Woodall, A. L. Sudlow, P. R. Raithby, G. Kociok-Köhn, K. C. Molloy and F. Marken, *Inorg. Chem.*, 2013,**52**, 12012-12022.
16. G. M. Sheldrick, *Acta Crystallogr., Sect. A*, 1990, **46**, 467.
17. G. M. Sheldrick, *Acta Crystallogr., Sect. A*, 2008, **64**, 112-122.
18. a) S.-S. Sun, D. T. Tran, O. S. Odongo and A. J. Lees, *Inorg. Chem.*, 2001, **41**, 132-135; b) J. T. Lin, S.-S. Sun, J. J. Wu, L. Lee, K.-J. Lin and Y. F. Huang, *Inorg. Chem.*, 1995, **34**, 2323-2333; c) J. T. Lin, S.-S. Sun, J. J. Wu, Y.-C. Liaw and K.-J. Lin, *J. Organomet. Chem.*, 1996, **517**, 217-226.

19. a) T. M. Figueira-Duarte, V. Lloveras, J. Vidal-Gancedo, A. Gegout, B. Delavaux-Nicot, R. Welter, J. Veciana, C. Rovira and J.-F. Nierengarten, *Chem. Commun.*, 2007, 4345-4347; b) L. Cuffe, R. D. A. Hudson, J. F. Gallagher, S. Jennings, C. J. McAdam, R. B. T. Connelly, A. R. Manning, B. H. Robinson and J. Simpson, *Organometallics*, 2005, **24**, 2051-2060.

20. a) Y. Miura, F. Shimizu and T. Mochida, *Inorg. Chem.*, 2010, **49**, 10032-10040; b) A. K. Diallo, J.-C. Daran, F. Varret, J. Ruiz and D. Astruc, *Angew. Chem. Int. Ed.*, 2009, **48**, 3141-3145.

21. M. A. S. Gohera and T. C. W. Mak, *Polyhedron*, 1998, **17**, 3485-3494.

22. a) J. A. Loch, M. Albrecht, E. Peris, J. Mata, J. W. Faller and R. H. Crabtree, *Organometallics*, 2002, **21**, 700-706; b) H. Nishiyama, S. Yamaguchi, M. Kondo and K. Itoh, *J. Org. Chem.*, 1992, **57**, 4306-4309.

23. a) N. Chawdhury, N. J. Long, M. F. Mahon, L.-l. Ooi, P. R. Raithby, S. Rooke, A. J. P. White, D. J. Williams and M. Younus, *J. Organomet. Chem.*, 2004, **689**, 840-847; b) P. Huang, B. Jin, P. Liu, L. Cheng, W. Cheng and S. Zhang, *J. Organomet. Chem.*, 2012, **697**, 57-64; c) K. R. Justin Thomas, J. T. Lin and Y. S. Wen, *Organometallics*, 2000, **19**, 1008-1012.

24. a) V. N. Nemykin, G. T. Rohde, C. D. Barrett, R. G. Hadt, C. Bizzarri, P. Galloni, B. Floris, I. Nowik, R. H. Herber, A. G. Marrani, R. Zanoni and N. M. Loim, *J. Am. Chem. Soc.*, 2009, **131**, 14969-14978; b) J. Jiao, G. J. Long, L. Rebbouh, F. Grandjean, A. M. Beatty and T. P. Fehlner, *J. Am. Chem. Soc.*, 2005, **127**, 17819-17831; c) J. A. Kramer and D. N. Hendrickson, *Inorg. Chem.*, 1980, **19**, 3330-3337.

25. a) F. A. Mautner and M. A. S. Goher, *Polyhedron*, 1998, **18**, 553-559; b) H. Gökce and S. Bahçeli, *Spectrochim. Acta, Part A*, 2012, **96**, 139-147; c) M. A. S. Goher and F. A. Mautner, *Polyhedron*, 2000, **19**, 601-606; d) R. J. H. Clark and C. S. Williams, *Inorg. Chem.*, 1965, **4**, 350-357.

26. Z. Yu and L. E. Brus, *J. Phys. Chem. A*, 2000, **104**, 10995-10999.

27. E. E. Zvereva, S. A. Katsyuba and P. J. Dyson, *Phys. Chem. Chem. Phys.*, 2010, **12**, 13780-13787.

28. Y.-F. Yuan, T. Cardinaels, K. Lunstroot, K. Van Hecke, L. Van Meervelt, C. Görller-Walrand, K. Binnemans and P. Nockemann, *Inorg. Chem.*, 2007, **46**, 5302-5309.

29. a) M. Ferrer, A. Gutiérrez, L. Rodríguez, O. Rossell, J. C. Lima, M. Font-Bardia and X. Solans, *Eur. J. Inorg. Chem.*, 2008, **2008**, 2899-2909; b) R. H. Naulty, M. P. Cifuentes, M. G. Humphrey, S. Houbrechts, C. Boutton, A. Persoons, G. A. Heath, D. C. R. Hockless, B. Luther-Davies and M. Samoc, *J. Chem. Soc., Dalton Trans.*, 1997, 4167-4174.

30. L. M. Engelhardt, P. C. Healy, J. D. Kildea and A. H. White, *Aust. J. Chem.*, 1989, **42**, 107.

31. a) J. Jiao, G. J. Long, F. Grandjean, A. M. Beatty and T. P. Fehlner, *J. Am. Chem. Soc.*, 2003, **125**, 7522-7523; b) H. Plenio, J. Hermann and A. Sehring, *Chem. Eur. J.*, 2000, **6**, 1820; c) A. Donoli, A. Bisello, R. Cardena, C. Prinzivalli and S. Santi, *Organometallics*, 2013, **32**, 1029-1036; d) B. H. Northrop, H.-B. Yang and P. J. Stang, *Chem. Commun.*, 2008, 5896-5908.

32. a) R. Horikoshi, T. Mochida and H. Moriyama, *Inorg. Chem.*, 2002, **41**, 3017-3024; b) R. Horikoshi, C. Nambu and T. Mochida, *Inorg. Chem.*, 2003, **42**, 6868-6875.

33. A. Diez, J. Fernandez, E. Lalinde, M. T. Moreno and S. Sanchez, *Dalton Trans.*, 2008, 4926-4936.

34. E. E. Engelman and D. H. Evans, *J. Electroanal. Chem. Interfacial Electrochem.*, 1993, **349**, 141.

35. F. Qiu, R. G. Compton, F. Marken, S. J. Wilkins, C. H. Goeting and J. S. Foord, *Analytical Chemistry*, 2000, **72**, 2362-2370.

36. a) R. Qiu, X. L. Zhang, R. Qiao, Y. Li, Y. I. Kim and Y. S. Kang, *Chem. Mater.*, 2007, **19**, 4174-4180; b) H. C. Shin and M. Liu, *Adv. Funct. Mater.*, 2005, **15**, 582-586; c) M. J. Siegfried and K.-S. Choi, *Angew. Chem. Int. Ed.*, 2008, **47**, 368-372; d) H. Choo, B. He, K. Y. Liew, H. Liu and J. Li, *J. Mol. Catal. A: Chem.*, 2006, **244**, 217-228.

37. a) C. Tanaka, J. Tanaka and M. Matsumoto, *Phys. Chem. Chem. Phys.*, 2011, **13**, 16005-16014; b) K. Kobayashi, S. Horiuchi, R. Kumai, F. Kagawa, Y. Murakami and Y. Tokura, *Phys. Rev. Lett.*, 2012, **108**, 237601.

38. a) A. Castro, C. Correas, O. Pena, A. R. Landa-Canovas, M. Alguero, H. Amorin, M. Dolle, E. Vila and T. Hungria, *J. Mater. Chem.*, 2012, **22**, 9928-9938; b) A. S. Tayi, A. K. Shveyd, A. C. H. Sue, J. M. Szarko, B. S. Rolczynski, D. Cao, T. J. Kennedy, A. A. Sarjeant, C. L. Stern, W. F. Paxton, W. Wu, S. K. Dey, A. C. Fahrenbach, J. R. Guest, H. Mohseni, L. X. Chen, K. L. Wang, J. F. Stoddart and S. I. Stupp, *Nature*, 2012, **488**, 485-489.

39. a) Y. Hong, C. Tian, B. Jiang, A. Wu, Q. Zhang, G. Tian and H. Fu, *Journal of Materials Chemistry A*, 2013, **1**, 5700-5708; b) W. L. Noorduin, A. Grinthal, L. Mahadevan and J. Aizenberg, *Science*, 2013, **340**, 832-837; c) E. Vlieg, *Science*, 2013, **340**, 822-823; d) M. Wang, G. Jiang, Y. Tang and Y. Shi, *CrystEngComm*, 2013, **15**, 1001-1006; e) J. Xu, C. Zhang, X. Wang, H. Ji, C. Zhao, Y. Wang and Z. Zhang, *Green Chemistry*, 2011, **13**, 1914-1922.

40. Y. Zhou and B. Yan, *CrystEngComm*, 2013, **15**, 5694-5702.

41. a) A.Thander, B.Mallik, *Indian Journal of Physics,* 2012, **86**, 521-528; b) M. Kurbanov, G. Suleymanov, N. Safarov, A. Gochuyeva, I. Orujov, Z. Mamedova, *Semiconductors,* 2011, **45**, 503-509

42. S. Horiuchi, Y. Tokunaga, G. Giovannetti, S. Picozzi, H. Itoh, R. Shimano, R. Kumai and Y. Tokura, *Nature*, 2010, **463**, 789-792.

43. a) S. L. McFarlane, B. A. Day, K. McEleney, M. S. Freund and N. S. Lewis, *Energy & Environmental Science*, 2011, **4**, 1700-1703; b) J. M. Tarascon, C. Delacourt, A. S. Prakash, M. Morcrette, M. S. Hegde, C. Wurm and C. Masquelier, *Dalton Trans.*, 2004, 2988-2994.

GRAPHICAL ABSTRACT

New Di-Ferrocenyl-Ethynylpyridinyl Triphenylphosphine Copper Halide Complexes and related Di-Ferricenyl Electro-crystallized Materials

H. H. Shah, R. A. Al-Balushi, M. K. Al-Suti, M. S. Khan, F. Marken, A. L. Sudlow, G. Kociok-Köhn, C. H. Woodall, P. R. Raithby and K. C. Molloy

Three new di-ferrocenyl-ethynylpyridinyl copper complexes, $[L_2(CuCl)_2(PPh_3)_2]$ (**2**), $[L_2(CuBr)_2(PPh_3)_2]$ (**3**), and $[L_2(CuI)_2(PPh_3)_2]$ (**4**) were synthesized from the ferrocenyl-ethynylpyridine. CV measurements show chemically reversible ferrocenyl oxidation signals followed by characteristic "stripping reduction peaks" indicating that oxidation-product electro-crystallization is occurring.